Hydrogen Assisted Cracking of Palladium Modified PH 13-8 Mo Stainless Steel

J.R. Scully, J.A. Van Den Avyle, M.J. Cieslak, C. R. Hills

Metallurgy Department
Sandia National Laboratories
Albuquerque, New Mexico, 87185

SAND--89-2413C

DE90 001501

Abstract

We compare the hydrogen assisted cracking resistance of wrought PH 13-8 Mo stainless steel alloyed with 0.4 to 1.0 wt.% palladium to the conventional alloy when aged to yield strengths of 1170-1250 MPa. Pd is found both in solid solution in the martensitic phase and also in the form of randomly distributed, incoherent PdAl precipitates in the modified alloy. Interfacial segregation of Pd to grain boundaries and lath boundaries is not observed. Intergranular hydrogen cracking is suppressed with Pd in slow strain rate tests conducted during electrochemical hydrogen charging of precharged samples. Hydrogen permeation analyses indicate that hydrogen ingress is not inhibited by Pd but that bulk diffusion rates are lowered relative to the conventional alloy. These results are consistent with the creation of a strong hydrogen trap, most likely the uniformly distributed PdAl phase, which lowers the levels of interfacially segregated hydrogen.

This work performed at Sandia National Laboratories supported by the U.S. Department of Energy under contract number DE-AC04-76DP00789

Introduction

Many ferrous based engineering alloys with yield strength levels exceeding 550 MPa (80 Ksi) are susceptible to hydrogen induced degradation of mechanical properties. Small palladium alloying additions reduce susceptibility to hydrogen assisted cracking in quenched and tempered AISI 4130 steel [1-3]. K_{ISCC} and threshold stress in sustained load tests are significantly improved [1-2]. The fracture surface is modified such that intergranular cracking is replaced by transgranular tearing and ductile microvoid formation [1-3] when 1 wt.% Pd is added to the martensitic alloy at both 745 MPa (110 ksi) [1-2] and 1170 MPa (170 ksi) [3] yield strength levels. The reported explanation for the improvement involves the interfacial segregation of Pd to interphase interfaces such as manganese sulfide inclusions and lath boundaries [4] which are otherwise strong trapping sites for hydrogen. Tritium autoradiography indicated the absence of tritium at MnS inclusions when complexed by segregated Pd [5]. The implication of these results, while not completely understood, is that Pd partitioning in the alloy can significantly alter the distribution of trapped interfacial hydrogen affecting resistance to embrittlement caused by hydrogen assisted interfacial decohesion.

Here, we report the influence of 0.39, 0.75, and 1.02 wt.% Pd added to wrought PH 13-8 Mo stainless steel (0.05% C, 0.10% Mn, 0.010% P, 0.01% P, 0.008% S, 0.10% Si, 13.25% Cr, 8.50% Ni, 1.35% Al, 2.50% Mo, Bal Fe), aged to the H-1050 condition (1170-1250 MPa yield strength). We compare the hydrogen assisted cracking resistance of these Pd modified alloys to the conventional alloy at the same yield strength.

Experimental

Pd additions were made to 3 heats of alloy PH 13-8 Mo. The Pd levels chosen correspond to two levels (0.75 and 1.02%) previously observed to improve hydrogen cracking resistance and one level (0.39%) which had no effect [1-2]. Chemical compositions and processing details are reported elsewhere [6]. Samples were aged to the H-1050 condition (565°C for 4 hours) producing the mechanical properties indicated in Table 1.

Auger spectroscopy was performed with a PHI Model 595 Scanning Auger Microscope operated at 3 KeV. Argon sputtering was conducted at 2 keV (SiO_2 sputter rate equal to 22 nm/minute). Analytical electron microscopy (AEM) was performed with a JEOL 2000 FX AEM equipped with a high take-off angle Tracor Northern EDS detector/spectrometer [6]. A Hitachi Model S-500 microscope was used for fractography.

Table 1. Tensile Properties of Pd-Modified PH 13-8 Mo*

Pd Content (wt.%)	0.2% Yield Stress ksi(MPa)	Ultimate Stress ksi(MPa)	Elongation (%)
0.0	181(1250)	186(1280)	15.8
0.39	184(1270)	188(1300)	16.9
0.75	180(1240)	185(1280)	17.3
1.02	170(1170)	179(1240)	18.9

* -- average of two tests after aging treatment at 565°C for 4 hr

Slow strain rate tests were conducted with circumferentially notched round bar specimens with a semicircular notch of radius equal to 0.07 cm and a notch diameter of 0.497 cm. Notch surfaces were polished. Specimens were strained to failure at $1x10^{-6}$ cm/second crosshead displacement rate in 0.6 M NaCl. Specimens were tested under continual cathodic polarization at -25 $\mu A/cm^2$ (-1.1 Volt vs. Saturated Calomel Electrode (SCE)) for 30 hours prior to commencement and during mechanical testing. These conditions have been observed to cause significant hydrogen assisted cracking in AISI 4340 steel at a similar yield strength [7].

Hydrogen permeation tests were conducted by galvanostatic electrochemical charging of 0.0254 cm thick specimens at -1.0 mA/cm^2 using the Devanathan-Stachurski technique [8]. Procedures discussed elsewhere were followed except that Pd was not utilized on the exit surface [9]. The exit surface was potentiostatically controlled at -600 mV vs. SCE (-0.1 $\mu A/cm^2$ background current density). "Steady state" diffusion coefficients (irreversible trap sites saturated) were determined at 15, 24, 40, and 64°C from linear regression analysis of initial permeation decay and second rise transients as explained elsewhere [9]. The initial rise transient was compared to subsequent "steady state" rise and decay transient data to investigate irreversible trapping [10].

Results

Metallurgy

PH 13-8 Mo is a low carbon martensitic stainless steel which transforms to martensite at relatively low temperature (M_S = 130°C, M_f = 20°C). Precipitation of the intermetallic phase, β-NiAl, occurs within the martensitic matrix in the temperature range of 425- 620°C. PH 13-8 Mo is austenitic above 800°C. Examination of as cast (vacuum-arc-remelted) PH 13-8 Mo showed that (a) Pd lowers the M_S temperature, (b) Pd was soluble and therefore favored partitioning into the austenitic phase of the duplex as-cast structure, and (c) 1 μm size PdAl precipitates (Pm3m structure) are formed in the ferrite phase of the duplex as-cast structure [6]. In the present examination of single phase (martensitic) wrought product, submicron sized PdAl precipitates were observed in the martensitic phase after the precipitation hardening heat treatment, as shown in Figure 1. These precipitates were uniformly distributed throughout the martensite and were not uniquely associated with either the prior austenite grain boundaries or the martensitic lath boundaries. These precipitates cause a slight decrease in post-aged yield strength at the 1% Pd level (Table 1). An AEM/EDS spectra obtained for one of these particles indicates high levels of both Pd and Al are present (Figure 2). Using the microchemical analysis capabilities of the AEM, grain and lath boundaries were analyzed for segregation of Pd. Segregation of Pd to austenitic grain boundaries during solutionizing is not anticipated as the microstructure is wholly austenitic and Pd is completely soluble. For the aged material, point probe analysis (20 nm probe) of randomly oriented boundaries in a 100-150 nm thick specimen showed a Pd concentration at the grain boundary statistically indistinguishable from the matrix.

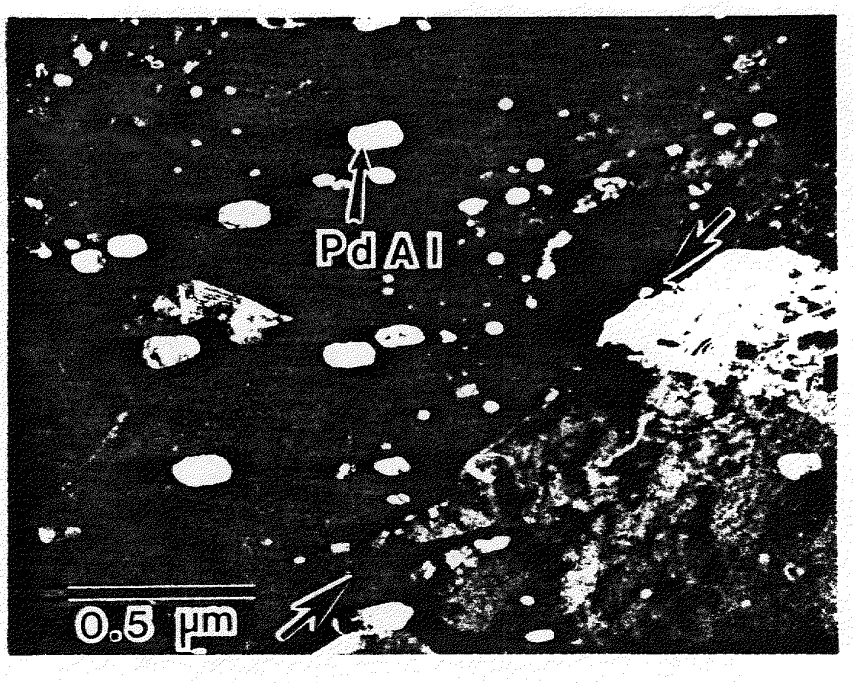

Figure 1. Transmission electron micrograph (dark field) of aged PH 13-8 Mo with 1% Pd showing random distribution of PdAl intermetallic phase. The arrows indicate the lath boundary.

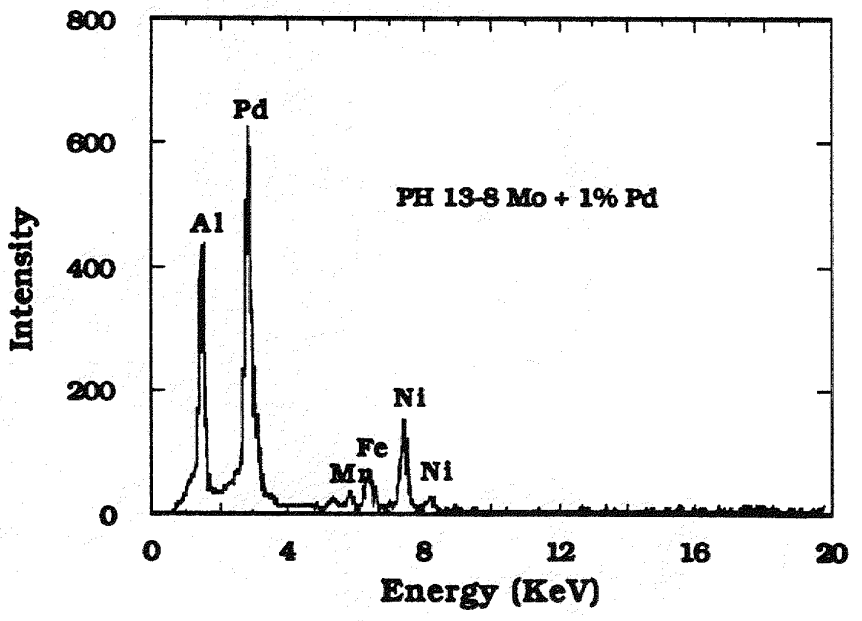

Figure 2. AEM/EDS spectra for PdAl precipitate

Environmental- Mechanical Behavior

The influence of Pd on mechanical properties in slow strain rate testing (SSRT) is shown in Figure 3. Here, hydrogen damage is expressed as the ratio of the maximum load attained in the SSRT to the same parameter obtained in a separate air test of replicate specimens. 1% Pd has a significant influence on the ratio. However, 0.39% Pd has only marginal benefit. Since the time to failure in these tests was 60-70 hours, hydrogen charging to obtain a uniform hydrogen distribution across the entire cross-section of the notched diameter was not obtained during this short time period (Based on diffusion coefficients determined below and calculated times required to obtain a uniform hydrogen concentration [7]). To verify that the Pd affect is operative after charging to steady state hydrogen concentrations an additional specimen (0.75% Pd) was cathodically charged in 0.1 M NaOH. This specimen was continually charged at -100 $\mu A/cm^2$ and did not fail after over 200 days with a sustained dead weight load which is greater than the maximum load observed for the conventional (0% Pd) alloy in the SSRT.

For specimens tested in air, 100% ductile microvoid coalescence fracture is observed on fracture surfaces. Intergranular cracking (Figure 4) on prior austenite grain boundaries is observed for the hydrogen charged 0% Pd alloy. This cracking extends from the root of the notch and is followed by microvoid coalescence characteristic of ductile overload in the center of the sample. For all of the alloys containing Pd, intergranular fracture is completely absent. Instead, hydrogen assisted cracking is transgranular with a tearing topography that is crystallographically consistent with interlath and translath tearing (Figure 5). Cracking extends from the root of the notch and transitions to microvoid coalescence characteristic of ductile overload in the center of the sample. Auger analysis for segregation of Pd to lath boundaries did not indicate Pd above the approximately 1% Pd present in solid solution. This was concluded after comparison of the Pd peak to peak heights (330 eV) obtained on individual laths of the fracture surface of the 1% Pd alloy to the Pd peak to peak height obtained while rastering the electron beam over a large area of the ductile overload fracture surface on the same sample.

Hydrogen Absorption and Permeation

Cathodic polarization data for the conventional alloy, the modified alloy, and 99.99% Pd in deaerated 0.6 M NaCl, pH=8 are shown in Figure 6. The cathodic Tafel slope and the exchange current density for the reduction of water reaction (obtained by extrapolating Tafel slopes to the reversible electrode potential, here -0.713 Volts vs. SCE) for both alloys are practically identical as compared to pure Pd. Pure Pd is observed to catalyze the hydrogen evolution reaction (H.E.R.)(despite the ability to absorb large quantities of hydrogen) as evident from the higher exchange current density. The surface concentration of Pd appears to be too low in the modified alloy to effectively lower the overpotential from that obtained with the conventional alloy. Auger analysis of the air formed oxide (accomplished by argon sputtering) and metal surface indicated no significant Pd enrichment. Corrosion and possible surface enrichment were suppressed during exposure in 0.6 M NaCl by cathodic polarization.

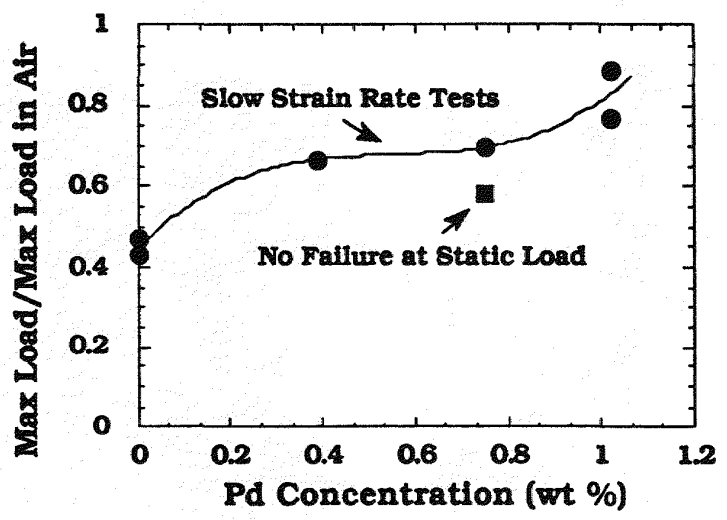

Figure 3. Influence of Pd concentration in PH 13-8 Mo stainless steel (H-1050) on the ratio of the maximum load in slow strain rate tests to the maximum load for duplicate specimens tested in air. For the static load test the applied load is utilized instead of maximum load.

Figure 4. Secondary electron micrograph of mostly intergranular fracture surface for conventional PH 13-8 Mo (H-1050) after slow strain rate testing.

Figure 5. Secondary electron micrograph of transgranular fracture surface for PH 13-8 Mo modified with 1% Pd (H-1050) after slow strain rate testing.

The steady state hydrogen permeation flux for the conventional and the modified alloy are shown in Figure 7 at various cathodic charging current densities. The flux is lower for the 1.0% Pd alloy in all cases. "Steady state" diffusion coefficients were determined at 15-64°C after attainment of initial steady state permeation fluxes (Figure 8). Since ideally irreversible traps are by then already saturated these diffusion coefficients are representative of the "apparent" impedance to diffusion in the presence of strong but reversible trapping sites and interstitial lattice sites [10]. The diffusion coefficients for the conventional alloy are greater than those for the Pd modified alloy at all temperatures. The data at 24°C explains the steady state permeation behavior (Figure 7) at the same temperature: The apparent diffusion coefficient for the conventional alloy is almost double that of the Pd modified alloy, and from Fick's first law this accounts for the observation that the steady state permeation flux is lower by almost half for the Pd modified alloy.

The initial permeation rise transient can be compared to the second permeation rise transient to obtain information on the density of traps and the degree to which trapping sites are irreversible and saturable. Long initial breakthrough times, long times to reach steady state, and lower apparent diffusion coefficients calculated from the initial rise transient are indicative of the influence of a high density of irreversible traps on the apparent impedance to diffusion. A summary of diffusion data at 15°C are shown in Table 2. The aged Pd modified alloy has the longest breakthrough time, lowest initial diffusion coefficient, and lowest steady state diffusion coefficient of all alloys.

Table 2. Summary of Apparent Diffusion Coefficients Determined at 15°C

Alloy	Breakthrough Time (seconds)	Initial D † (cm^2/sec)	Steady State D †† (cm^2/sec)
PH 13-8 Mo	1.36×10^4	2.7×10^{-9}	5.2×10^{-9}
PH 13-8 Mo (1) with 1% Pd	$1.83 \times 10^{4*}$	$1.5 \times 10^{-9*}$	$2.9 \times 10^{-9*}$
PH 13-8 Mo (2) with 1% Pd	0.67×10^4	5.5×10^{-9}	$7.0 \times 10^{-9*}$

(1) aged, (2) solutionized
* -- average of two tests
† -- irreversible traps not saturated, †† -- irreversible traps saturated

Discussion

The addition of Pd to aged PH 13-8 Mo is observed to decrease hydrogen diffusion coefficients and, therefore, permeation compared to the conventional alloy. Concomitant with this modification is a decrease in hydrogen induced interfacial decohesion at prior austenite grain boundaries. There are three mechanisms possible. These are (a) inhibited

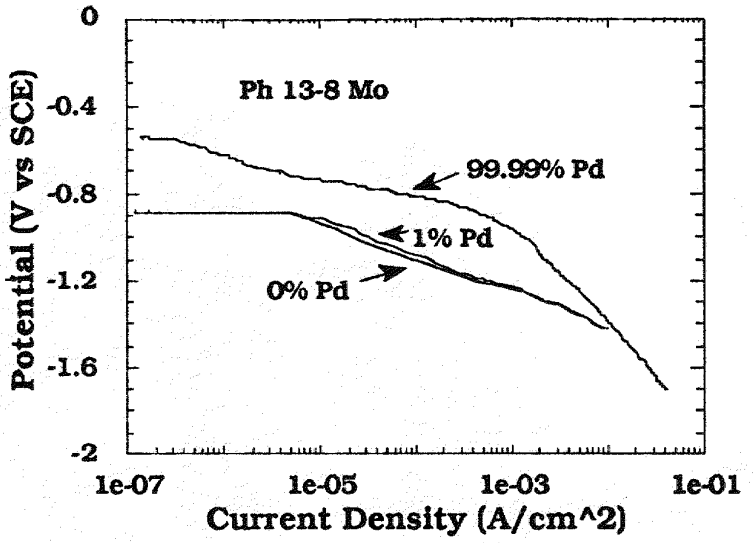

Figure 6. Cathodic polarization behavior of conventional PH 13-8 Mo, Pd modified PH 13-8 Mo, and 99.99% Pd in 0.6 M NaCl.

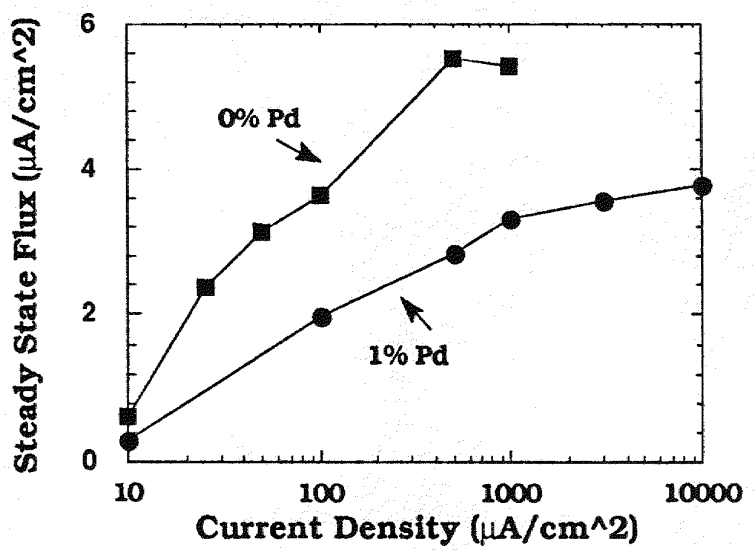

Figure 7. Relationship between cathodic charging current density and steady state hydrogen permeation flux for conventional PH 13-8 Mo and Pd modified PH 13-8 Mo in 0.6 M NaCl solution at 24°C.

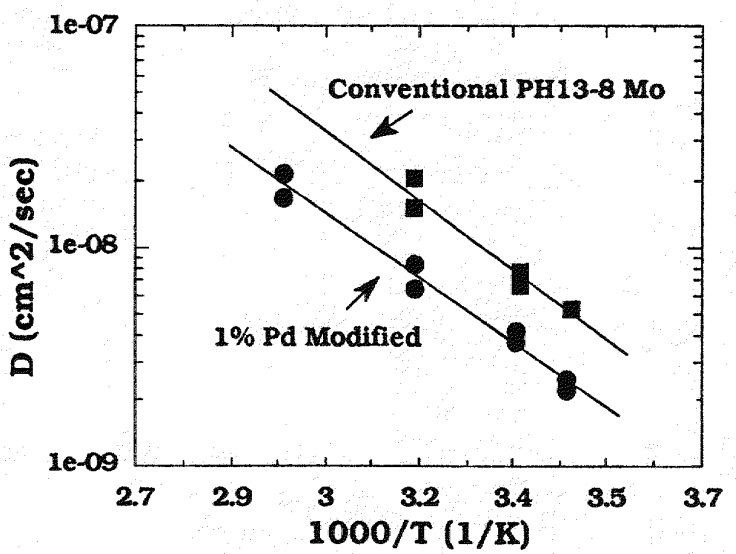

Figure 8. Relationship between steady state diffusion coefficients representative of reversible trapping and reciprocal temperature over the range of 24 to 64°C for conventional PH 13-8 Mo and Pd modified PH 13-8 Mo in 0.6 M NaCl solution.

hydrogen ingress, (b) elemental Pd segregation to interfaces and repulsion of hydrogen at the same, and (c) formation of strong reversible traps that diminish hydrogen segregation to interfaces at a given hydrogen fugacity because of a redistribution of occluded hydrogen in the presence of such traps. One alternative mechanism concerns the possibly that Pd retards segregation of decohesion promoting elements to grain boundaries during aging. While this secondary role is not implicated in the present work, it cannot be entirely dismissed without further investigation. Mechanism (a) is dismissed for the following reasons. For low alloy steels in seawater the mechanism of H.E.R. is coupled discharge-chemical recombination [9]. For this reaction mechanism the surface coverage of adsorbed hydrogen, θ, will increase with exchange current density, i_o, Tafel slope, β_{ca}, and hydrogen overpotential, η, as follows [9].

$$\theta = \{i_o/2FK_{des}\}^{0.5} \cdot \exp\{-\beta_{ca}\eta\, F/2RT\} \qquad (1)$$

Here, K_{des} is the reaction constant for recombinative desorption and other terms are given elsewhere [9]. Assuming first order reaction kinetics, hydrogen absorption should increase with increasing coverage. Both the conventional and the modified alloy have almost the same values for i_o, β_{ca}, and, consequently, η at the same current density. A decrease in hydrogen surface coverage (Equation 1) is not expected with 1.0% Pd. Consequently, 1% Pd is not expected to inhibit hydrogen ingress. The decrease in permeation rates is fully attributable to a decrease in bulk diffusion. In regard to mechanism (b), significant segregation of Pd to metallurgical interfaces was not detected using AEM. The possible role of interfacial segregated Pd in amounts lower than detected in the present experiments can not be entirely ruled out. Concerning mechanism (c), the permeation data strongly suggests that that there is a high density of traps in the aged modified alloy that absorb hydrogen both irreversibly and reversibly but are not saturated under the conditions studied. If such traps were irreversible and saturated, the steady state diffusion data would be the same for both the aged Pd modified alloy and the conventional alloy after the initial charging filled these irreversible traps. Table 2 contains data from the 1% Pd modified alloy after a solutionizing heat treatment but without aging. Both PdAl and β-NiAl precipitates are absent. Pd exists in solid solution in the martensitic phase. This specimen has the greatest diffusion coefficients under all conditions. This implies that Pd in solid solution is not a strong trap and that PdAl is the strong reversible trap observed in the aged Pd modified alloy. The influence of PdAl on diffusion is in accordance with trapping theory [11]:

$$D_{app} = D_{con}/(1 + kN/p) \qquad (2)$$

where D_{app} and D_{con} are the "steady state" diffusion coefficients for the modified and conventional alloys, respectively, N is the trap density, k the trapping rate, and p the trap release rate. The following ranking of reversible trap binding energies, E, can be deduced analogous to the role of elemental Ti in solid solution in iron [12].

$$E(PdAl\text{-}H) > E(GB\text{-}H),\ E(\beta\text{-}NiAl) > E(lattice\text{-}H)$$

Ti additions in iron are observed to suppress intergranular cracking by lowering the hydrogen concentration at grain boundaries [12]. Here, we

hypothesize that the reversible PdAl traps play a similar role. Pd substitutional solid solution atoms appear to be either weak traps or repel hydrogen. Elements which are located to the right of iron in the periodic table of the elements (Pd) should repel hydrogen when present in solid solution as sole atoms while elements to the left of iron (Ti) should trap hydrogen [13,14]. The exact nature of the reversible PdAl trap, e.g. physical, attractive, or mixed in nature [15] is unclear. Future work is underway to address these questions.

Acknowledgements

The authors wish to acknowledge F. Bovard for performing electrochemical experiments, W. Buttry for conducting Auger analyses, and A. Romig for reviewing the manuscript. We would also like to thank F. Zanner, R. Fisher and the staff of the Sandia National Laboratories Melting and Solidification Facility for preparing the alloys.

References

1. B. E. Wilde, C.D. Kim, and J.C. Turn Jr., Corrosion, 38(10)(1982), 515-524.
2. J.B. Lumsden, B.E. Wilde, and P.J. Stocker, Scripta Met., 17(1983), 971-974.
3. B.E. Wilde, I. Chattoraj, T.A. Mozhi, Scripta Met., 21(1987), 1369-1373.
4. M.K. Miller, S.S. Brenner, M.G. Burke, Met Trans A, 18A(1987), 519-523.
5. T. D. Le, and B.E. Wilde, In Current Solutions to Hydrogen Problems in Steels, Proceedings of First International Conference, Eds. C.G. Interrante, G.M. Pressouyre, American Society for Metals, Metals Park, Ohio, (1982), 413-422.
6. M.J. Cieslak, J.A. Van Den Avyle, C.R. Hills, R.E. Semarge, Met Trans A, 19A(1988), 3063-3069.
7. J.R. Scully, P.J. Moran, Corrosion, 44(3)(1988), 130-192.
8. M.A.V. Devanathan, Z. Stachurski, Proc. R. Soc. (London), 270A(90) (1962).
9. J.R. Scully, P.J. Moran, J. Electrochem. Soc., 135(6)(1988), 1337-1348.
10. G.M. Pressouryre, F.M. Faure., In Hydrogen Embrittlement: Prevention and Control, ASTM STP 962, L. Raymond, Ed., American Society for Testing and Materials, Philadelphia, (1988), 353-371.
11. R.A. Oriani, Acta Met., 18(1970), 147-157.
12. G.M. Pressouyre and I.M. Bernstein, Acta Met., 27(1979), 89-100.
13. G.M. Pressouyre, Met Trans A, 14A(1983), 2189-2193.
14. A.I. Shirley, C.K. Hall, Scipta Met., 17(1983), 1003-1008.
15. G.M. Pressouyre, Met Trans A, 10A(1979), 1571-1573.